Chinese Chemical Letters 35 (2024) 108936

Contents lists available at ScienceDirect

Chinese Chemical Letters

journal homepage: www.elsevier.com/locate/cclet

C14-HSL limits the mycelial morphology of pathogen *Trichosporon* cells but enhances their aggregation: Mechanisms and implications

Xin Lu[a], Haoran Sun[a], Xiaomeng Li[a], Chunrui Li[a], Jinfeng Wang[b], Dandan Zhou[a,*]

[a] *Jilin Engineering Lab for Water Pollution Control and Resources Recovery, School of the Environment, Northeast Normal University, Changchun 130117, China*

[b] *State Key Laboratory of Pollution Control and Resource Reuse, School of the Environment, Nanjing University, Nanjing 210023, China*

ARTICLE INFO

Article history:
Received 25 April 2023
Revised 10 August 2023
Accepted 14 August 2023
Available online 18 August 2023

Keywords:
Bacterial C14-HSL
Mycelium
Cell cycle
Aggregation
Aromatic proteins

ABSTRACT

The biosecurity hazards caused by pathogenic fungus have been widely concerned. Given the long-term coexistence of eukaryotic pathogens and quorum sensing bacteria in different habitats in environments, we hypothesized that they have social interactions *via* signal molecules. In this work, we firstly discovered the well-known bacterial signal molecules play an adverse role in the cell morphology and metabolism in a model pathogen *Trichosporon asahii*. *N*-Tetradecanoyl-L-homoserine lactone (C14-HSL) was discovered to increase pathogen hazards of *T. asahii*, which limited mycelium by 52%, but enhanced cell aggregation by 93%. Higher fluorescence intensity of tryptophan (59%) and aromatic protein (2-fold) contents after the treatment of C14-HSL, indicating that aromatic proteins helped aggregate *Trichosporon* and showed hydrophobicity. Transcriptome analysis revealed that C14-HSL upregulated the shikimate pathway (above 1-fold) located in downstream of tricarboxylic acid cycle, which contributed to the synthesis of more aromatic proteins and the formation of larger flocs. The limited mycelial growth of *T. asahii* attributed to the up-regulated expressions of cell cycle process. The fungal transboundary response to bacterial C14-HSL was controlled by signal transduction pathways. This study provides new insights into the co-evolution of bacterial and pathogenic fungi in microecosystems.

Over the past decade, invasive infections caused by opportunistic fungal pathogens have dramatically emerged in immunocompromised patients, which were considered as a serious public health problem [1–3]. The pathogenic fungus is widely distributed in nature areas, and infect the human body as yeast form through the bloodstream, when medical devices were invaded the human body [4–7]. In such microecosystem, fungi coexisted with neighbor bacteria to form a strong aggregation on the surface of prosthetic devices, which embedded in an extracellular polymeric substance (EPS), resulting in more severe infections [8]. Therefore, transboundary interactions between pathogenic fungi and bacteria are probably of great significance and ultimately lead to pathogenicity and human infections.

Just like human society, the sophisticated cell–cell communication systems also are developed in multicellular kingdom for allowing to gather and share of critical information [9–11]. The co-evolution of fungi and bacteria can be regulated by chemical signal molecules, which achieve their ecological niches in multi-species coexisting environments [9].

N-Acyl-homoserine lactones (AHLs) are classical signal molecules that synthesized by Gram-negative bacteria [10]. AHLs have potential function for kingdom communication between bacteria and fungi, due to varieties structures with a common lactonized homoserine moiety with different length acyl chain from 4 to 18 carbons and their modified by a 3-oxo substituent or a 3–hydroxy substituent [11]. Numerous studies have been reported that pathogenic *Candida albicans* were almost entirely in the yeast morphology in the presence of high concentrations of *N*-dodecanoyl-L-homoserine lactone (C12-HSL) and 3-oxo-C12-HSL (40 μmol/L) [12–14]. In addition to morphological effects, transboundary signal molecule transduction can also affect the production of extracellular polymeric substances (EPSs), thus changing eukaryote harvesting and aggregation [9,15]. Coincidentally, C10-HSL, 3-oxo-C10-HSL, and 3-OH–C10-HSL (0.1 mg/L) were reported to improve the production of diatomaceous EPS [15]. *Galactomyces geotrichum* also sensed bacterial C10-HSL (5 μmol/L) and increased spore germination rates by 22% and carbohydrate production by 1.0–2.5 folds [9]. Whereas, fungal pathogens form

* Corresponding author.
E-mail address: zhoudandan415@163.com (D. Zhou).

https://doi.org/10.1016/j.cclet.2023.108936
1001-8417/

aggregations by producing EPS, resulting in the risk of severe infections [8].

For pathogenic yeast-like *Trichosporon*, disseminated trichosporiasis infections possess 42%–90%, despite antifungal therapy [6]. It seems *Trichosporon* always exists in the same circumstances that enrich bacteria, implying its evolutionary development may be connected to bacterial cells [16]. However, how *Trichosporon* response to bacterial signal molecules is unknown. we deduced that the above transboundary interactions may regulate its physiological characters by bacterial signaling molecules, such as the well-known AHLs.

In our proof-of-concept study, 19 AHL species were added into pure *Trichosporon* cultivation to obverse their biological responses to bacterial AHLs. Only long-chained *N*-tetradecanoyl-L-homoserine lactone (C14-HSL) was discovered to significantly inhibit hyphae length and evaluate mycelium aggregation based on Student's *t*-test, thus we choose C14-HSL as specific AHLs that acts on the kingdom interaction between bacteria and pathogenic fungi. Further, the effect of C14-HSL on EPS components and a physiological metabolic model of *T. asahii* were elaborated to reveal the effect of various mechanisms on the pathogen's morphology and accumulation *via* cross-border coevolution. This work firstly explores the synergistic interaction between pathogenic fungi and co-exited bacteria, which provide novel understanding on caring of life and health.

Strains of the model yeast *T. asahii* were purchased from China General Microbiological Culture Collection Center (CGMCC) and were subcultured on sabouraud dextrose agar (Haibo Biotechnology Co., Ltd., Qingdao, China) at 37 °C [17]. In all experimental protocols, single cells were obtained by fabric filtration and transferred to Stoke's medium (1 g/L glucose, 1 g/L peptone, 0.2 g/L $MgSO_4{\cdot}7H_2O$, 0.05 g/L $CaCl_2$ and 0.01 g/L $FeCl_3$) at 28 °C with an inoculation concentration of 10^6 spores/mL [18]. Commercial AHLs standards were purchased from Sigma Corporation. All experimental groups were treated with 500 nmol/L 19 signal molecules (including C14-HSL), and the control group was not treated with AHLs.

Cell morphology was observed under an optical microscope (BX53, Olympus, Japan). The length of mycelial cells was observed and recorded using a photographic system (DS-U3). Referring to Sun *et al*., 10 microscopic images were selected from each experiment to calculate the average mycelium [1]. In addition, the morphological features of aggregates were assessed using Image Pro Plus 6.0 software (Media Cybernetics, US) [19]. All experiments were performed three times, and the results were expressed as the mean ± standard deviation. The collected images were processed with contrast, color saturation, and hue-saturation-intensity (HSI) measurement of the area selection. The fractal dimension (D_f) and hole ratio (HR) were built-in software parameters. The area (A) and F_{max} were measured to calculate the compactness (*Comp*, Eq. 1).

$$Comp = \frac{\sqrt{\frac{4}{\pi}A}}{F_{max}} \tag{1}$$

Extracellular protein components were extracted using a heating method in which samples were heated at 60 °C for 30 min, then centrifuged at 4 °C at 10,000 rpm for 10 min [20]. The protein content in the membrane-filtered supernatant (0.45 μm, cellulose acetate) was determined using a Folin-phenol kit (Dingguo Bioengineering Institute, Beijing, China) [21]. Amino acid-like substances were analyzed according to fluorophores using excitation-emission matrix spectroscopy (EEM) that was divided into five spectra regions (Region I: tyrosine protein with Ex/Em = 200–250/200–250 nm, Region II: aromatic protein Ex/Em = 200–250/250–380 nm, Region III: Fulvic acid Ex/Em = 200–250/380–450 nm; Region IV: tryptophan protein Ex/Em = 250–350/200–380 nm; Region IV: polysaccharide Ex/Em = 250–350/380–450 nm) [22]. EEM analysis was performed with a fluorospectrometric photometer (RF-6000, Shimadzu, Japan) with a scanning speed of 6000 nm/min and emission and excitation spectral width of 200–500 nm, with an emission/emission slit bandwidth of 5 nm [23]. The data of the EEM spectra were pretreated to eliminate disturbances from Rayleigh and Raman scattering using MATLAB software [24]. The area of the protein component peaks was quantified by fluorescence region integration (FRI). Fluorescence data were processed using Origin 2021 software.

According to Yu *et al*., the effect of C14-HSL on the flocculation ability (FA, Eq. 2) of the protein fraction in a kaolin suspension was determined [25]. The mixtures were composed of a protein fraction (0.1 mL), 90 mmol/L, $CaCl_2$ (0.25 mL), and 5 g/L kaolin suspension (4.65 mL). They were allowed to stand for 5 min after being vortexed for 30 s. The OD_{550} of the protein fraction in the experiment (OD_{550}) and control ($OD_{550,\,a}$) were determined using an ultraviolet and visible (UV–vis) spectrophotometer (TU-1901, Persee, China).

$$FA = \frac{OD_{550,a} - OD_{550}}{OD_{550,a}} \times\ 100\% \tag{2}$$

To investigate whether C14-HSL affected the surface properties of *T. asahii*, relative hydrophobicity (RH, Eq. 3) was determined by the adsorption of hexadecane to a strain [26]. A 5 mL sample was vortexed for 30 s, and OD_{600} was measured as I_0. Hexadecane (1 mL) was added to the sample, and the mixture was rotated for 2 min and allowed to rest for 10 min. The OD_{600} of the aqueous phase (I) was measured after extraction separation.

$$RH = \frac{I_0 - I}{I_0} \times\ 100\% \tag{3}$$

Samples with and without C14-HSL were centrifuged at 10,000 ×g for 10 min, and then the particles were immediately frozen in liquid nitrogen and then sent to Novogene Ltd. (Beijing, China) for RNA extraction. Fungal RNA extraction details were performed according to the manufacturer's protocol. Average RNA samples (1.5 μg) were collected for RNA-seq library construction (NEBNext® Ultra™ RNA Library Prep Kit, Illumina®, NEB, USA). Quality control was performed for each RNA-seq library based on default parameters through Agilent Bioanalyzer 2100 system (Agilent Technologies, CA, USA). The library preparations were sequenced on an Illumina Novaseq platform and 150 bp paired-end reads were generated. To ensure high-quality data, reads containing adapter, reads containing ploy-N, and poor-quality reads were removed from the raw data. The final transcriptome assembly was subjected to transcriptome data analysis using Trinity's default parameters and reference genomic methods [27]. Differential gene expression analysis expressed upregulated and downregulated genes as defined by the log2-fold change, logFC > 1 and logFC < 1 [28], respectively. Gene function annotations were referenced and assigned using the Kyoto encyclopedia of genes and genomes (KEGG) database by the GhostKOALA server (http://www.kegg.jp/ghostkoala/). The raw RNA sequences were uploaded on the GSA database (https://ngdc.cncb.ac.cn/gsa/) with accession number CRA011764.

As shown in Table 1, C14-HSL was identified as the functional signal molecules that had a significant effect on the morphology and aggregation of *T. asahii* from 19 widely-investigated AHL species. C14-HSL inhibited mycelium growth, and the average length of mycelium decreased by 52% from 91. 61 ± 1.96 μm to 55.87 ± 0.99 μm (n = 10). The D_f value increased significantly from 1.27 to 1.81, the porosity decreased significantly from 55% to 10%, and compactness increased significantly from 55% to 88%. Despite the inhibition of fungal mycelium, the increased aggregation indicated that C14-HSL potentially enhanced fungal biofilm formation and attachment, thus enhancing the hazards of pathogenic fungi. C14-HSL is a long-chain AHLs secreted by Gram-negative bacteria

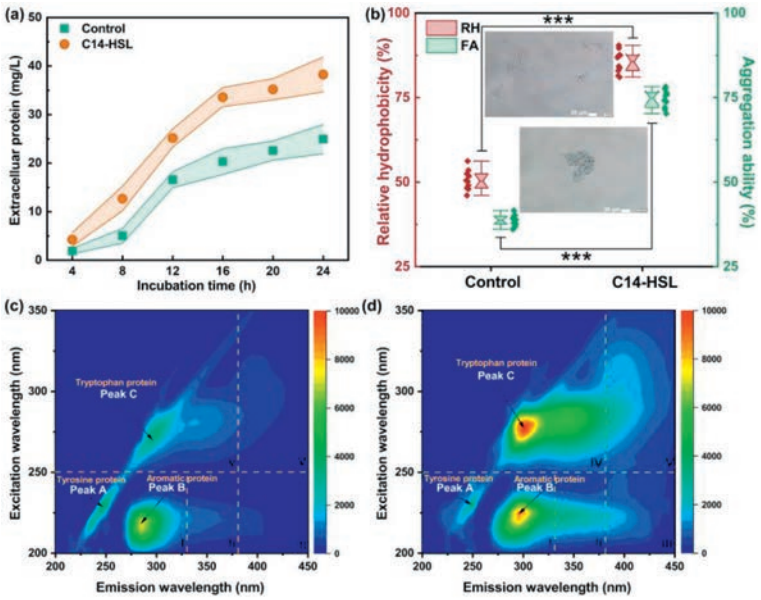

Fig. 1. Comparison of extracellular protein contents and surface hydrophobicity of *T. asahii* in the absence and presence of C14-HSL. (a) Extracellular protein production; (b) surface hydrophobicity and aggregation ability variations (inset images represent the fungal pellets in the control and C14-HSL, respectively); (c, d) EEM spectra of *T. asahii*'s extracellular components in the absence and presence of C14-HSL.

Table 1
Effects of 19 selected AHLs on the hyphal length and fungal aggregation morphology.

Category	Hyphal length	D_f	HR (%)	Comp (%)
Control	91. 61 ± 1.96	1.27±0.12	55.21±1.38	55.35±1.23
C4-HSL	95.21 ± 1.89	1.29 ± 0.15	56.58 ± 1.02	54.07 ± 1.18
3-oxo-C4-HSL	89.23 ± 1.98	1.31 ± 0.21	54.59 ± 1.25	56.89 ± 1.27
3OH–C4-HSL	90.11 ± 1.21	1.26 ± 0.13	55.69 ± 1.58	58.71 ± 1.08
C6-HSL	91.35 ± 1.59	1.28 ± 0.18	58.36 ± 1.78	56.57 ± 1.25
3-oxo-C6-HSL	92.31 ± 1.18	1.29 ± 0.25	57.31 ± 1.57	57.39 ± 1.49
3OH–C6-HSL	95.01 ± 1.76	1.27 ± 0.19	55.78 ± 1.79	57.96 ± 1.36
C7-HSL	94.35 ± 1.47	1.28 ± 0.28	53.89 ± 1.27	54.86 ± 1.24
C8-HSL	93.04 ± 1.25	1.31 ± 0.27	56.87 ± 1.88	56.85 ± 1.53
3-oxo-C8-HSL	90.56 ± 0.94	1.29 ± 0.16	58.51 ± 1.67	58.75 ± 1.74
3OH–C8-HSL	91.36 ± 0.86	1.28 ± 0.35	57.79 ± 1.81	55.54 ± 1.88
C10-HSL	95.34 ± 1.37	1.30 ± 0.19	56.36 ± 1.57	57.97 ± 1.36
3-oxo-C10-HSL	93.78 ± 1.15	1.29 ± 0.26	55.75 ± 1.04	56.19 ± 1.23
3OH–C10-HSL	94.54 ± 1.09	1.31 ± 0.34	57.19 ± 1.31	58.34 ± 1.19
C12-HSL	95.65 ± 1.42	1.29 ± 0.22	58.97 ± 1.19	57.36 ± 1.71
3-oxo-C12-HSL	93.37 ± 1.29	1.30 ± 0.58	55.43 ± 1.61	58.59 ± 1.62
3OH–C12-HSL	91.89 ± 1.47	1.31 ± 0.39	57.66 ± 1.25	56.58 ± 1.25
C14-HSL	55.87 ± 0.99	1.81 ± 0.55	10.39 ± 0.63	88.69 ± 1.95
3-oxo-C14-HSL	91.57 ± 1.08	1.29 ± 0.46	58.39 ± 1.53	55.48 ± 1.19
3OH–C14-HSL	93.68 ± 1.72	1.31 ± 0.61	55.36 ± 1.37	57.76 ± 1.47

Table 2
Half-volume peaks of EEM spectrum with and without C14-HSL.

Peak	Peak intensity		Peak area	
	Control	C14-HSL	Control	C14-HSL
Peak A	4291.23	4002.57	1.69×10^6	1.73×10^6
Peak B	7282.95	8508.00	7.42×10^6	11.81×10^6
Peak C	3647.39	9944.78	6.69×10^6	19.52×10^6

and exist in bacteria-related symbiotic microecosystems, such as water, air, and soil environments [4–6].

As shown in Fig. 1, 37% more extracellular protein was produced by *T. asahii* when there was trace C14-HSL stimulation after 24 h. Fungal aggregation is a process that involves hydrophobic interactions and may result in protein enrichment [9]. We further found that the surface hydrophobicity of cells increased by 69%. EEM results revealed that the proteins were tryptophan (region I) and aromatic proteins (region VI) (Fig. 1). Table 2 shows that C14-HSL increased tryptophan and aromatic protein intensity by 59% and 2-fold, respectively. These regulation mechanisms are native self-protection characteristics of yeast cells under environmental stress. Sun *et al.* also found that phenethyl alcohol induced yeast cell aggregation by producing more aromatic and tryptophan proteins [1]. Likewise, other study also found that bacterial AHLs stimulated microalgae to secrete aromatic proteins so that they formed considerable microalgal pellets [15]. In this work, C14-HSL caused *T. asahii* physicochemical properties to change in such a way that promoted the accumulation of yeast; thus, the flocculation ability of the pathogen increased by 93%. This implied that the wide occurrence C14-HSL-producing bacteria, such as *Citrobacter amalonaticus* [29], *Rhodobacter capsulatus* [30] and *Nitrosospira multiformis* [31], significantly increased the hazards of *T. asahii*.

Fig. 2 shows the elongation of related polypeptides involved in aromatic protein synthesis. The synthesis of aromatic proteins originating from the tricarboxylic acid cycle began with the oxidation of acetyl-coenzyme A (CoA), which was mainly produced *via* the shikimate pathway [32]. This dynamic process involved the synthesis of L-tryptophan, L-phenylalanine, L-tyrosine, and aromatic amino acids [11]. Differentially-expressed genes encoding synthase after C14-HSL stimulation were upregulated (1.03–6.32 fold) compared with the controls. These findings implied that the ability of *T. asahii* to secrete aromatic amino acids was promoted by C14-HSL signals. These extracellular proteins constituted the hydrophobic fraction of EPS, allowing the structure of bioaggregates to be constructed and maintained [33–35]. And, the synthesis and secretion of amino acids can alter the surface hydrophobicity of mycelia and accelerate the aggregation of fungal mycelial [2,14]. These results directly indicate that *T. asahii* could sense typical bacterial signal molecules, C14-HSL, and showed either cell surface modulation or metabolic regulation.

The cell cycle process determines *T. asahii* growth toward yeast or mycelia formation, which includes the first gap (G1) phase, synthesis (S) phase, second gap (G2) phase, and mitosis. Combined, these constitute the whole process from DNA replication to cell reproduction [36]. Fig. 3 illustrates that up-regulation of *Cdc28* ex-

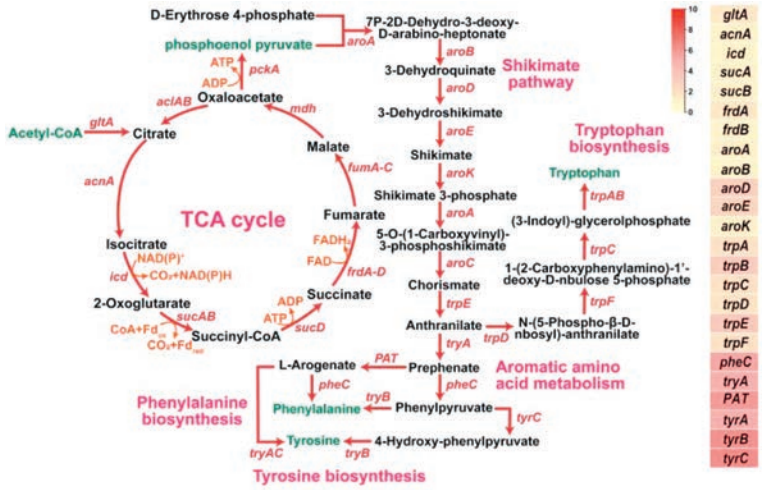

Fig. 2. Aromatic amino acid and tryptophan biosynthesis and metabolism pathway of *T. asahii* under stimulation by C14-HSL. The expressions of genes were plotted in heat map, which was inserted in metabolic pathways. The redder the color, the higher the levels of up-regulated expressions (control *vs*. C14-HSL).

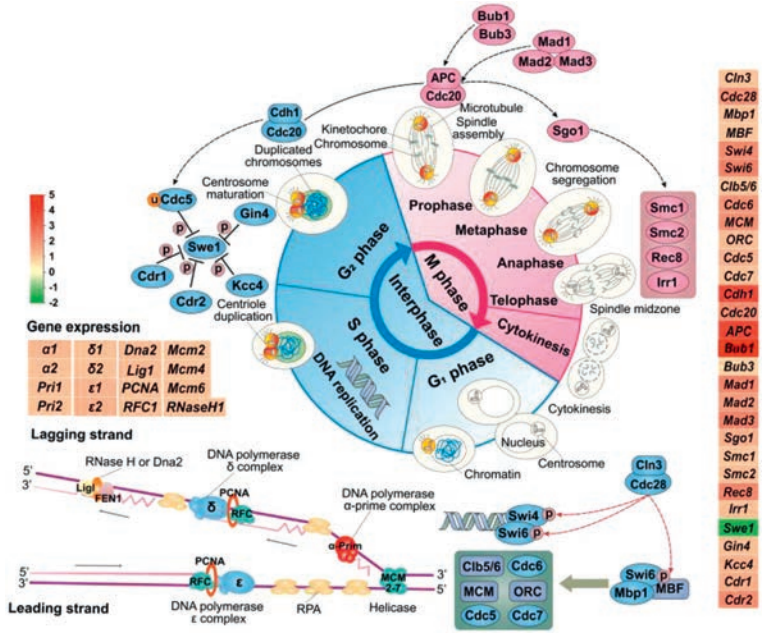

Fig. 3. The regulation of C14-HSL on cell cycle entry and DNA replication. The inserted gene heat maps on the left and right represent the gene expressions in the cell cycle and DNA replication, respectively. The expressions of genes were plotted in heat map, which was inserted in metabolic pathways. The red represents up-regulation, and green represents down-regulation (control *vs*. C14-HSL).

pression (1.99-fold) triggered the activity expressions of cell cycle regulatory mechanisms (>1-fold). Genes involved in the G1 phase, such as *Swi4*, *Swi6*, *Mbp1*, *MBF*, *MCM* and *ORC*, were positively expressed between 1.09 and 2.38 fold when stimulated by bacterial C14-HSL. The results showed that C14-HSL activated the transition from the G1 phase to the S phase during preparation for DNA reproduction in yeast cells. During the S phase, the up-regulation of gene cluster expression (1.04–2.01 fold) showed that the treatment of C14-HSL promoted DNA synthesis, and yeast cells started to enter the mitosis stage. Meanwhile, the up-regulated expressions (1.12–2.13 fold) of genes (*e.g.*, *Cdc5*, *Gin4*, *Cdr1*, *Cdr2* and *Kcc4* in the G2 phase) that responsible for inhibiting Swe1 also supported above result, which results in the down-regulated expressions of Swe1, indicating that yeast cells completed the interphase. C14-HSL activated the signal sensor *Cdc28*, then up-regulated the expressions of its downstream genes, such as *Swi4*, *Swi6*, *Cdc5*, *Cdc7*, *etc*., which are responsible for DNA replication and promoting the initial stage of the cell cycle. After C14-HSL treatment, all genes involved in mitosis were up-regulated (0.99–6.57 fold). The results showed that C14-HSL promoted spindle assembly, chromosome segregation, spindle midzone, and cell division, thus enabling complete yeast cell division. Extracellular chemical signals influence the decision to enter S phase through activating G1 phase, then DNA is replicated, which is intrinsically linked with cell proliferation [37,38]. DNA replication is central to cell growth and ensure the process of cell cycle to complete cell division, resulting in inhibiting mycelial formation [39]. Thus, C14-HSL promoted the proliferation of more yeast cells and inhibited the formation of mycelia in *T. asahii*.

In yeast, β-oxidation provides energy for oxidative phosphorylation and produces acetyl-CoA for ketogenesis in the mitochondrial matrix [40]. As shown in Fig. 4, β-oxidization-related genes, such as *FadD*, *ACOX1*, *HADH*, *FadA* and *ACAT*, were up-regulated by 1.13-6.17 fold. Gene clusters encoding oxidative phosphorylation

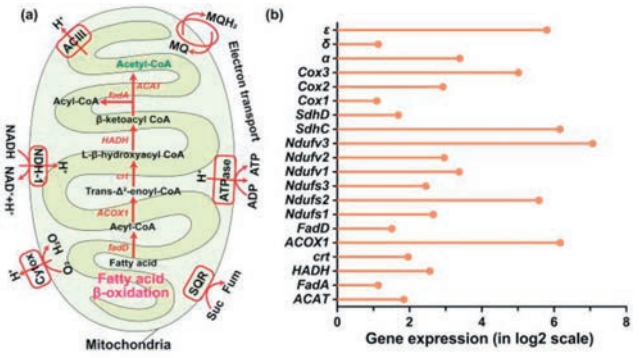

Fig. 4. (a) C14-HSL regulates the mitochondria to activate oxidative phosphorylation and fatty acid β-oxidation in *T. asahii*. (b) The up-regulation of C14-HSL in differential genes associated with oxidative phosphorylation and fatty acid β-oxidation (Control *vs.* C14-HSL).

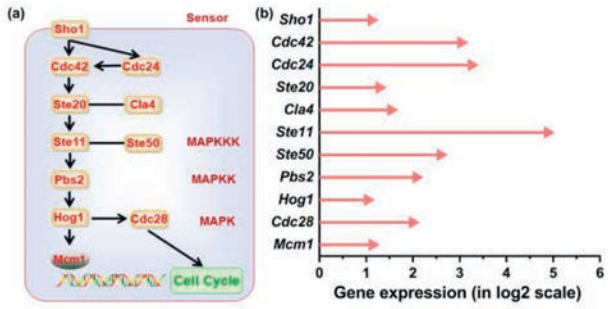

Fig. 5. (a) The specific signal transduction in *T. asahii* to respond to bacterial C14-HSL and (b) differential-expression associated genes (control *vs.* C14-HSL).

were upregulated in response to C14-HSL stimulation (1.09–6.16 fold). These results indicated that C14-HSL promoted the complete degradation of all fatty acids through mitochondrial metabolism, which generated more adenosine triphosphate (ATP) for oxidative phosphorylation to promote cell reproduction and growth. More importantly, acetyl-CoA, derived from fatty acid β-oxidation, played an important role in promoting amino acid metabolism through the tricarboxylic acid cycle [41]. Up-regulation of the expression of *Suc* and *Fum* confirmed the depletion of ATP during the tricarboxylic acid cycle. As a result, bacterial C14-HSL stimulated the mitotic and metabolic activity of ATP-supplement in yeast cells. The up-regulation of oxidative phosphorylation activated the upstream β-oxidation of fatty acids, followed by the citric acid cycle.

Mitogen-activated protein kinase (MAPK), MAP kinase kinase (MAPKK), and MAP kinase kinase kinase (MAPKKK) are important signaling pathways by which yeast cells respond and adapt to external signal stimuli [42]. Extracellular signals bind to specific receptors on the membrane surface and then trigger the central module *via* an intermediate protein [43]. Gene clusters *Ste1*, *Pbs2*, *Hog1* and *Cdc28*, which are responsible for sensing environmental stress in *T. asahii*, were more than 1-fold upregulated (Fig. 5). These results suggest that C14-HSL activated the signaling pathway of quorum sensing (QS) bacterial neighbors. The positive expression of the signaling receptor gene *Sho1* (1.11-fold) confirmed that *T. asahii* could perceive bacterial signal molecules and that there was cross-border coevolution between them. A 1.03-fold upregulation of Hog1 expression was observed. *Hog1* plays an important role in regulating the cell wall structure, negatively affecting yeast's transition to a mycelial morphology [44]. This explains why C14-HSL inhibited *T. asahii* mycelial growth. Furthermore, after activation of *Hog1*, *Pbs2* was also upregulated (2.07-fold), suggesting that C14-HSL weakened the filaments of *T. asahii* and inhibited cell wall changes. These transcriptome results reveal the signaling pathway of C14-HSL in bacteria, which prevented the overexpression of mycelium.

T. asahii is an opportunistic microbial pathogen that infects various hosts, such as humans, plants, and animals, *via* the overgrowth and aggregation of fungal mycelium [4–6]. Fungi and bacteria co-colonize and co-exist in microhabitats; therefore, transboundary interactions between microbiota members contribute to the establishment, stability, and resilience to the environmental factors of hosts [14,45]. In this study, a functional AHL secreted by bacterial cells was shown to be important for the overgrowth and aggregation of fungal mycelium through a cell-cell communication pattern. Bacterial C14-HSL increased the expression of genes associated with the biosynthesis of tryptophan and aromatic proteins, which formed larger fungal mycelium aggregations by secreting many more extracellular proteins. More conclusively, C14-HSL blocked the transformation of the mycelial morphology by up-regulating the expression of cell cycle processes with the activation of the signal receptor gene *Sho1*. Recently, a technology aimed to block or disturb the QS signaling pathway through coordinating the expression of targeted genes, called quorum quenching (QQ), has proven promising for keeping the balance between fungi and bacteria in microecosystems [14,45]. The 3-oxo-C12-HSL was also discovered to inhibit the formation of various fungal mycelium and biofilms by mimicking the farnesol inhibitory pathway [14]. The discovery of existing natural signals act on the co-evolution microbial interaction across boundary provide clues for precisely controlling pathogenic infections in the future.

This study showed that bacterial C14-HSL inhibited the mitosis of *Trichosporon* and its morphological transformation from yeast to mycelium. The cells became highly hydrophobic and accumulated. Transcriptome analysis revealed that C14-HSL promoted the synthesis of aromatic proteins and limited cell cycles and enhanced energy metabolism *via* signal transduction pathways. Taken together, these results showed that *T. asahii* could undergo cross-border communication with C14-HSL-producing bacteria, but this increased the pathogen's potential hazards. These results show that bacterial signal molecules can be employed to block or disturb fungal metabolism to treat pathogenic infections in microecosystems.

Declaration of competing interest

The authors declare that they have no known competing financial interests or personal relationships that could have appeared to influence the work reported in this paper.

Acknowledgments

The authors thank the National Natural Science Foundation of China (Nos. 52070036, U20A20322), and the Fundamental Research Funds for the Central Universities (No. 2412018ZD042) for their financial support.

References

[1] J. Sun, H. Sun, W. Lv, et al., J. Environ. Chem. Eng. 9 (2021) 105817.
[2] R.A. Cordeiro, A.L.R. Aguiar, V.S. Pereira, et al., Microb. Pathog. 130 (2019) 219–225.
[3] H.X. Zhao, T.Y. Zhang, H. Wang, et al., Sci. Total Environ. 853 (2022) 158626.
[4] A.L. Colombo, A.C.B. Padovan, G.M. Chaves, et al., Clin. Microbiol. Rev. 24 (2011) 682–700.
[5] E.R. Galligan, L. Fix, S. Husain, et al., J. Cutan. Pathol. 46 (2019) 159–161.
[6] A. Subramanian, S. Devi, G. Abraham, et al., Med. Mycol. Case Rep. 35 (2022) 15–17.
[7] T.L. Han, R.D. Cannon, S.G. Villas-Bôas, Fungal Genet. Biol. 48 (2011) 747–763.
[8] G.D. Bonaventura, A. Pompilio, C. Picciani, et al., Antimicrob. Agents Chemother. 50 (2006) 3269–3276.
[9] X. Lu, Y. Wang, Z. Feng, et al., Chin. Chem. Lett. 34 (2023) 107617.

[10] J. Shuai, X. Hu, B. Wang, et al., Chin. Chem. Lett. 32 (2021) 3402–3409.
[11] S. Li, P.H.M. Leung, X. Xu, C. Wu, Chin. Chem. Lett. 29 (2018) 313–316.
[12] L.D. Sordi, F.A. Mühlschlegel, FEMS Yeast Res. 9 (2009) 990–999.
[13] A. Davis-Hanna, A.E. Piispanen, L.I. Stateva, et al., Mol. Microbiol. 67 (2008) 47–62.
[14] J. Barriuso, D.A. Hogan, T. Keshavarz, et al., FEMS Microbiol. Rev. 42 (2018) 627–638.
[15] C. Yang, S. Fang, D. Chen, et al., Mar. Pollut. Bull. 107 (2016) 118–124.
[16] F. Getzke, T. Thiergart, S. Hacquard, Curr. Opin. Microbiol. 49 (2019) 66–72.
[17] Y. Liao, H. Zhao, X. Lu, et al., Med. Mycol. 53 (2015) 396–404.
[18] G. Gillot, N. Decourcelle, G. Dauer, et al., Food Microbiol. 57 (2016) 1–7.
[19] H. Fan, X. Liu, H. Wang, et al., Chemosphere 169 (2017) 586–595.
[20] Y. Sun, K. He, Q. Yin, et al., J. Environ. Sci. China 69 (2018) 85–94.
[21] Y. Shen, D.M. Huang, Y.P. Chen, et al., Sci. Total Environ. 712 (2020) 135795.
[22] P. Zhang, F. Fang, Y.P. Chen, et al., Chemosphere 117 (2014) 59–65.
[23] Q. He, J. Zhang, S. Gao, et al., Bioresour. Technol. 294 (2019) 122151.
[24] Z.P. Wang, T. Zhang, Water Res. 44 (2010) 5499–5509.
[25] G.H. Yu, P.J. He, L.M. Shao, Bioresour. Technol. 100 (2009) 3193–3198.
[26] R.S. Pembrey, K.C. Marshall, R.P. Schneider, Appl. Environ. Microbiol. 65 (1999) 2877–2894.
[27] C. Strub, C.A.T. Dieye, P.A. Nguyen, et al., Fungal Biol. 125 (2021) 78–88.
[28] E.K. Palonen, S. Raina, A. Brandt, et al., Microorganisms 5 (2017) E12.
[29] H.L. Kher, T. Krishnan, V. Letchumanan, et al., Gene 684 (2019) 58–69.
[30] A.L. Schaefer, T.A. Taylor, J.T. Beatty, et al., J. Bacteriol. 184 (2002) 6515–6521.
[31] N. Wang, J. Gao, Y. Liu, et al., Chemosphere 274 (2021) 129970.
[32] P.F. Fitzpatrick, Biochemistry 42 (2003) 14083–14091.
[33] Y. Li, W. Hao, J. Lv, et al., Bioresour. Technol. 159 (2014) 305–310.
[34] M. Pivokonsky, J. Naceradska, T. Brabenec, et al., Water Res. 84 (2015) 278–285.
[35] Y. Wang, H. Xu, H. Yao, et al., J. Hazard. Mater. 443 (2023) 130306.
[36] V.K. Gupta, O. Chaudhuri, Trends Cell Biol. 32 (2022) 773–785.
[37] R. Duronio, Y. Xiong, Cold Spring Harb. Perspect. Biol. 5 (2013) a008904.
[38] D. Patzelt, H. Wang, I. Buchholz, et al., ISME J. 7 (2013) 2274–2286.
[39] G. Zou, K. Zhang, W. Yang, et al., Chin. Chem. Lett. 32 (2021) 3252–3256.
[40] J. Frankovsky, V. Vozáriková, J. Nosek, et al., Mitochondrion 57 (2021) 148–162.
[41] Q. Zhang, W. Zeng, S. Xu, et al., Bioresour. Technol. 342 (2021) 125978.
[42] D. Martínez-Soto, J. Ruiz-Herrera, Rev. Iberoam. Micol. 34 (2017) 192–202.
[43] J. Zhou, Y. Lyu, M. Richlen, et al., Crit. Rev. Plant Sci. 35 (2016) 81–105.
[44] R. Alonso-Monge, E. Román, D.M. Arana, et al., Clin. Microbiol. Infect. 15 (Suppl. 1) (2009) 17–19.
[45] S.A. Padder, R. Prasad, A.H. Shah, Microbiol. Res. 210 (2018) 51–58.